Zinc/Iron mixed-metal MOF-74 derived magnetic carbon nanorods for the enhanced removal of organic pollutants from water

Mateo del Rio, Juan Carlos Grimalt Escarabajal, Gemma Turnes Palomino, Carlos Palomino Cabello**

Department of Chemistry, University of the Balearic Islands, Palma de Mallorca, E-07122, Spain.

*E-mail: carlos.palomino@uib.es *E-mail: g.turnes@uib.es Fax: (+34) 971 173426 Phone: (+34) 971173389

KEYWORDS: Mixed-metal MOFs; magnetic porous carbon; extraction of pollutants; water treatment; phenols

ABSTRACT

The preparation of magnetic porous carbon from a mixed-metal-organic framework by a two steps simple method is reported. By taking advantage that the calcination process at high temperature under inert atmosphere of zinc and iron MOFs results in the formation of carbons with excellent porosity and magnetic properties, respectively, MOF-74(Zn/Fe) prepared at room temperature was used as precursor for the synthesis of high porous magnetic carbons. The prepared materials were characterized by XRD, FTIR spectroscopy of adsorbed CO, SEM, TEM, N_2 adsorption-desorption, Zeta potential analysis and energy dispersive X-ray spectroscopy. To check the potential as sorbent of the MOF-74(Zn/Fe)-derived magnetic porous carbon, adsorption isotherms of methylene blue and methyl orange were recorded and compared with those obtained using a non-magnetic MOF-74(Zn)-derived porous carbon. The maximum adsorption capacity for methylene blue and methyl orange was 370 and 239 mg g^{-1}, which are higher than those reported for other magnetic adsorbents. The study of the extraction performance of the dyes at different pH, along with Zeta potential analysis, revealed that electrostatic and π-π interactions might be involved in the dyes removal. C-MOF-74(Zn/Fe) material showed good reusability with no apparent loss in dye extraction capacity after five cycles and the ability to treat large volume of dye polluted water. In addition, the developed C-MOF-74(Zn/Fe) showed excellent performance for the simultaneous removal of different endocrine disrupting phenols (bisphenol A, 4-tert-butylphenol and 4-tert-octylphenol) from water, demonstrating that mixed-metal-organic frameworks are promising precursors for the preparation of a wide number of new porous materials.

1. INTRODUCTION

Water is one of the most important natural resources for life and the sustainability of the environment. At present, the intensification of human activities and the rapid progress of modern industry have resulted in water contamination with a variety of different organic pollutants, including hormones, pesticides, phenols, dyes, and personal care and hygiene products, which represents an important worldwide environmental problem [1, 2]. Therefore, the development of treatment technologies that allow to achieve the elimination of these organic pollutants and guarantee the quality of the treated waters is of great importance. Different physical and chemical methods, such as membrane separation [3-5], adsorption [6-8], Fenton oxidation [9], coagulation [10], and photodegradation [11] have been used for the remediation of wastewater. Among them, due to its efficiency, low cost and simplicity, adsorption using porous materials as sorbents has emerged as one of the most attractive methods for water decontamination [12-15]. Various porous solids such as zeolites [16], activated carbons [17], silica-based mesoporous materials [18] and hydrotalcites [19] have been evaluated. The adsorption of organic pollutants by these materials occurs through a number of different mechanisms, including hydrophobic interactions, electrostatic interactions, hydrogen bonding, acid-base interactions, π–π stacking, or a combination of them [20-22].

Metal-organic frameworks (MOFs) are porous crystalline coordination compounds based on the coordination of metal ions or clusters with organic linkers to form 1D, 2D or 3D networks [23, 24]. Due to the large amount of metals and organic bridging linkers, along with the possibility of their chemical functionalization and of introducing more than one metal, organic linker, or mixtures of both, MOFs are becoming a rapidly growing family of nanoporous materials [25-27].

Due to their ultrahigh porosity and very high surface areas, tailored chemical functionalities, flexibility, and versatility, MOFs have been explored as sorbents for the extraction of different pollutants [28-30]. Two limiting factors for the application of MOFs in this field are their limited stability in aqueous or complex mediums and their laborious recovery after the extraction in batch conditions, which requires long centrifugation and filtration steps.

MOFs have been already used as precursors to obtain advanced porous carbons with uniform pores of different sizes and with novel structures and properties [31-33]. By direct MOF carbonization under inert atmosphere, where the precursor MOF functions as an efficient carbon source and template, porous carbon structures doped with heteroatoms coming from the linker can be obtained, in which the metal ions or clusters remains as metal or metal oxide nanoparticles distributed in the carbonaceous structure [34, 35]. MOF-derived carbons show active sites and high specific surface area and porosity, with the advantage, over the precursor MOFs, of being chemically more stable. These properties, along with an increase in favorable interactions with aromatic rings of organic compounds, make these porous solids very interesting and promising materials for the extraction of organic pollutants from water. For instance, zinc metal-organic framewoks, such as ZIF-8, have demonstrated to be efficient precursors to prepare nanoporous carbons since the use of high temperatures during the calcination process removes the zinc metallic centers and gives rise to porous carbons with excellent porosity [36]. ZIF-8-derived carbons have shown good performance in the removal of methylene blue dye [36, 37], diuron herbicide [38] and sulfamethoxazole [39] and ciprofloxacin [40] antibiotics. The potential of the porous carbons derived from Bio-MOF-1 and MAF-6 metal-organic frameworks as sorbents for removal of bisphenol A has also been studied and demonstrated by Bhadra et al. [41, 42]. Other examples of the use of MOFs-derived porous carbons for the extraction of organic pollutants are the application

of UiO-66 derived carbon for the removal of carbamazepine [43] and rhodamine B [44] from water and the use of MIL-125 for the extraction of phenols in water samples [45]. In addition, taking into account that the calcination process of the MOF results in the formation of metal- or metal oxide-carbon composite solids, the use of MOFs with different metallic centers as precursors allows to obtain porous carbon with different properties. So, for instance, the use of iron or cobalt metal-organic frameworks as precursors gives rise to magnetic porous carbons, which facilitates their retrieval by simply using an external magnet after their application for pollutants extraction in batch conditions [46-48]. However, the porosity of these carbons, a key factor for their use as adsorbents, is reduced by the presence of the metallic nanoparticles into the pore cavities of the carbons [46, 49].

Bearing this in mind, we report the use of a mixed-metal-organic framework as precursor to prepare magnetic porous carbon nanorods with high specific surface area by a simple two steps method and their application for the adsorption of organic pollutants. Zinc/iron mixed-metal MOF-74 (MOF-74(Zn/Fe)), prepared at room temperature, has been used as a precursor, in which iron provides magnetic properties and the selective removal of zinc by an easy calcination process provides high porosity to the resulting material. Methyl orange and methylene blue, common dye pollutants from the paper and textile industry, were selected as model adsorption analytes to study the extraction capacity of the prepared porous carbons. Additionally, the potential applicability of the developed material for the simultaneous extraction of endocrine disrupting phenols (bisphenol A, 4-tert-butylphenol and 4-tert-octylphenol) from water was also evaluated.

2. EXPERIMENTAL SECTION

2.1. Materials

Zinc acetate (Acros Organics, 99%), iron(II) acetate (Aldrich, 95%), 2,5-dihydroxyterephtalic acid (TCI, 98%), salicylic acid (Scharlau, 99,5%), N,N-dimethylformamide (Scharlau, >99%), methanol (PanReac-AppliChem, >99%) and acetonitrile (Scharlau, HPLC grade) were obtained from commercial sources and used as received. For the extraction experiments, methylene blue (Panreac, 99%), methyl orange (Fluka, 99%), bisphenol A (Aldrich, 97%), 4-tert-butylphenol (Aldrich, 99%) and 4-tert-octylphenol (Aldrich, 97%) were used. All solutions were prepared using Mili-Q water (Direct-8 purification system, resistivity > 18 MΩ cm, Millipore Iberica, Spain) or acetonitrile HPLC grade.

2.2. Characterization

Powder X-ray diffractograms were registered by using CuKα radiation on a Bruker D8 Advance diffractometer. The morphology of the prepared materials was studied by using a scanning electron microscope (Hitachi S-3400N), equipped with a Bruker AXS Xflash 4010 EDS system and transmission electron microscope (Hitachi ABS) operated at 100 kV. Thermogravimetric analysis (TGA) was carried out in an air atmosphere using a TA Instrument SDT 2960 simultaneous DSC-TGA. Nitrogen adsorption isotherms were measured at 77 K using a TriStar II (Micromeritics) gas adsorption analyzer. All samples were activated at 433 K for 16 h prior to measurement. Data were analyzed using the Brunauer-Emmett-Teller (BET) and non-local density functional theory (2D-NLDFT) models to determine the specific surface area and pore size distribution. The point of zero charge for the adsorbents was determined by employing a Zetasizer Nano ZS90 (Malvern). For IR experiments, a thin self-supported wafer of the MOF sample was prepared and degassed inside an IR cell under dynamic vacuum at 453 K for 8 h. After this thermal treatment, Fourier transform infrared (FTIR) spectra of the MOF samples, before and after carbon monoxide adsorption, were recorded using a Bruker Vertex 80v spectrophotometer working at 3 cm^{-1} resolution to study the

metal centers of the samples. Chromatographic experiments were performed by using a Jasco HPLC instrument composed of a high-pressure pump (PU-4180), a manual injector, and a photodiode array detector (MD-4017). The separation of phenol compounds was performed at room temperature on a C18 SpeedCore column (100 mm x 3 mm i.d. 2.6μm) by using a mobile phase composed of 75% of acetonitrile and 25% of water at a flow rate of 0.25 mL min^{-1}. The analytes were detected at λ=229.

2.3. Synthesis of MOF-74(Zn/Fe)

MOF-74 metal-organic framework was synthesized by adapting a procedure described in a previous report [50]. Typically, 3.13 g of anhydrous zinc acetate and 0.35 g of iron(II) acetate dissolved in 200 mL of DMF were added dropwise under constant stirring to 0.99 g of 2,5-dihydroxyterephthalic acid dissolved in 200 mL of DMF. After 5 min of additional stirring, a solution of salicylic acid (0.55 g) in DMF (50 mL) was added slowly with constant stirring, that was maintained for 15 min. After this time, the mixture was kept without stirring at room temperature for 30 min. The solid formed was filtered and washed 3 times with DMF and methanol, and then soaked in methanol at 393 K for 36 h. Finally, the solid was filtered and then dried at room temperature under vacuum, obtaining 2.6 g of the material.

For comparison, MOF-74(Zn) was prepared, following identical synthetic conditions as those used for the preparation of MOF-74(Zn/Fe), replacing the mixture of anhydrous zinc acetate and iron(II) acetate by 3.48 g of anhydrous zinc acetate.

2.4. Synthesis of MOF-derived carbons

The porous carbons C-MOF-74(Zn/Fe) and C-MOF-74(Zn) were obtained by direct carbonization of the synthesized MOF-74(Zn/Fe) and MOF-74(Zn), respectively, in a furnace under a nitrogen

atmosphere at 1273 K (heating rate of 2.5 K min^{-1}) for 3 h. From 1 g of MOF-74(Zn/Fe), 0.25 g of C-MOF-74(Zn/Fe) was obtained. The preparation method is summarized in Figure 1a.

2.5. Extraction experiments

The methyl orange and methylene blue extraction experiments were carried out in aqueous solution under batch conditions. Adsorption isotherm experiments were conducted in a concentration range of 100-800 mg L^{-1} of dye during 24 h to ensure that equilibrium conditions were reached. The remaining concentration of methyl orange and methylene blue in solution after extraction was measured using UV-Vis spectrophotometry at 466 nm and 664 nm, respectively. The maximum adsorption capacity was determined using the linearized form of the Langmuir equation [51], which is commonly represented as:

$$\frac{C_e}{q_e} = \frac{C_e}{q_{max}} + \frac{1}{q_{max}k}$$

where C_e (mg L^{-1}) is the remaining pollutant concentration at equilibrium, q_e (mg g^{-1}) is the amount of pollutant adsorbed at equilibrium (mg g^{-1}), q_{max} is the maximum adsorption capacity (mg g^{-1}), and k is the Langmuir constant (L mg^{-1}).

Simultaneous sorption capacity of the prepared porous carbons toward endocrine disrupting micropollutants was studied using 10 mL of a solution of phenol compounds (50 mg L^{-1}, each) after 24 h of extraction. The concentration of the pollutants remaining after extraction was measured by HPLC.

All the extraction experiments were performed in triplicate with the following conditions: sorbent concentration = 1.0 mg mL^{-1}; pH = 7.5; stirring = 500 rpm; room temperature; extraction time = 24 h. A schematic of the extraction procedure is shown in Figure 1b.

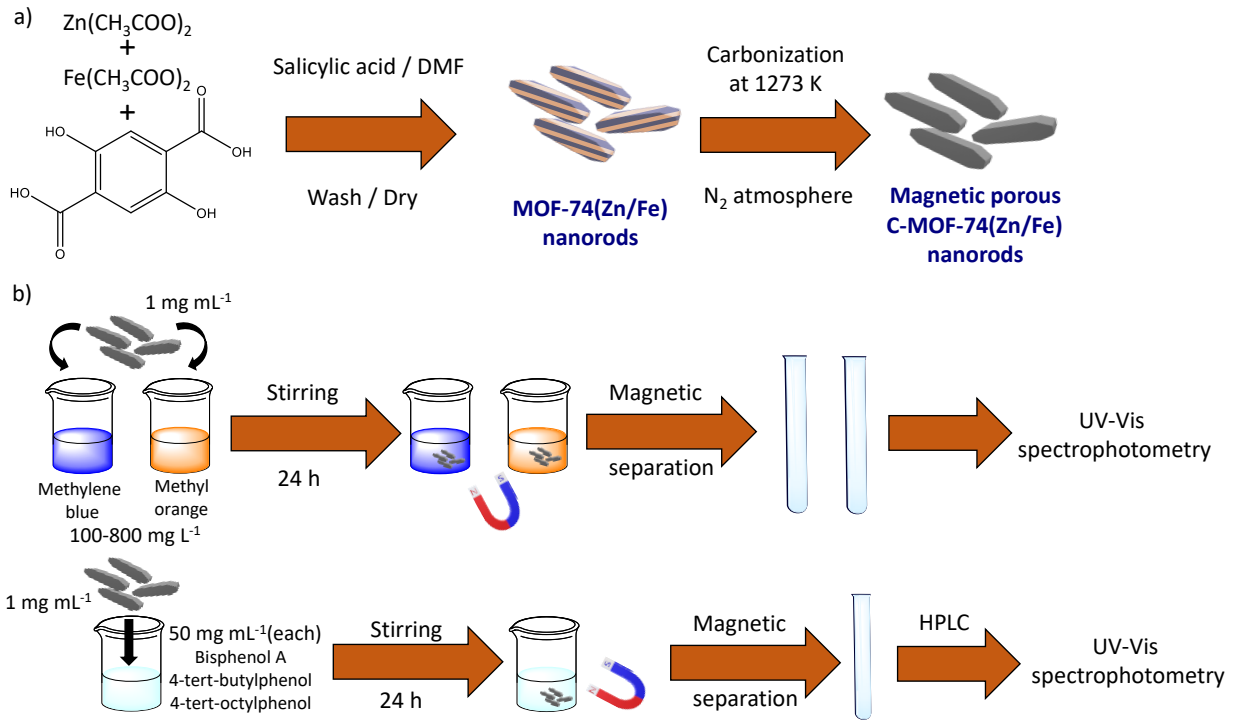

Figure 1. (a) Schematic representation of the preparation of magnetic porous C-MOF-74(Zn/Fe) nanorods. (b) Extraction procedure of dyes and phenolic compounds.

3. RESULTS AND DISCUSSION

3.1. Synthesis and characterization of MOF-74 precursors

In a first step, zinc/iron mixed-metal MOF-74 nanocrystals were prepared at room temperature. For comparison purposes, a zinc MOF-74 sample was also synthesized. The powder X-ray diffraction patterns of both MOF samples (Figure 2a) showed good crystallinity and were in good agreement with the XRD pattern previously reported for the MOF-74 structure [52]. The presence of zinc and iron in the MOF-74(Zn/Fe) sample was demonstrated by EDS (Figure S1). The EDS spectrum of the MOF-74(Zn/Fe) shows four bands at 6.4, 7.05, 8.6 and 9.6 KeV, which correspond to Fe (K_α and K_β) and Zn (K_α and K_β) peaks, respectively. Furthermore, the elemental EDS mapping (Figure S1) also shows the homogeneous distribution of both metals, Zn and Fe, in the

MOF-74(Zn/Fe) material. The incorporation of Zn and Fe cations in the structure of MOF-74(Zn/Fe) sample was studied by FTIR spectroscopy of adsorbed carbon monoxide at 100 K. The IR spectra of CO adsorbed on activated MOF-74(Zn/Fe) and MOF-74(Zn) samples are shown in Figure 2b. The infrared spectrum of adsorbed CO on MOF-74(Zn) shows a distinctive IR absorption band at 2172 cm^{-1}, which, in agreement with previous results by Bloch et al. [53], is assigned to the υ(CO) vibration mode of CO interacting (through the carbon atom) with coordinatively unsaturated Zn(II) cations of MOF-74. The IR spectrum of CO adsorbed on the MOF-74(Zn/Fe) sample shows a broad IR band in the CO stretching region which, as revealed by computer deconvolution, consists of two components centred at 2172 cm^{-1} and 2160 cm^{-1}. The band at 2172 cm^{-1}, as in the case of MOF-74(Zn) sample, corresponds to the CO adsorbed on the zinc cations, and the band at 2160 cm^{-1} is assigned to CO molecules interacting with the coordinatively unsaturated Fe(II) cations of MOF-74 [53], confirming the obtention of a zinc/iron mixed-metal MOF-74 material. The morphology of the prepared MOF-74 samples was studied by scanning and transmission electron microscopy (Figure 2c-d and Figure S2). As it can be observed, both samples were formed by nanometer-sized particles (20-40 nm wide and 100-300 nm long) with rod-shaped morphology, due to the addition into the reaction mixture of salicylic acid, that acts as modulator directing MOF growth [50].

3.2. Synthesis and characterization of MOF-74 derived porous carbons

By one-step carbonization of the MOF-74 precursors at 1273 K under inert atmosphere, porous carbons were obtained. Figure 3a shows the X-ray powder diffraction patterns of both, C-MOF-74(Zn/Fe) and C-MOF-74(Zn), carbon samples. After the carbonization, no X-ray diffraction peaks attributed to MOF-74 were observed in both cases, while two new broad bands appeared at $2\theta = 25$ and 42° in the diffractogram of C-MOF-74(Zn), indicating a certain graphitic degree of

the obtained carbon [34]. In the case of C-MOF-74(Zn/Fe), new diffraction lines (2θ > 35°) were observed, which were attributed to body-centered cubic α-Fe phase (JCPDS No. 06-0696) and to iron carbide (JCPDS No. 89-2867) [54-57]. The absence of peaks related to metallic zinc and other zinc compounds in the X-ray diffraction patterns of both carbons suggested the in situ removal of Zn (boiling point, 907 °C) during the carbonization process [50, 58].

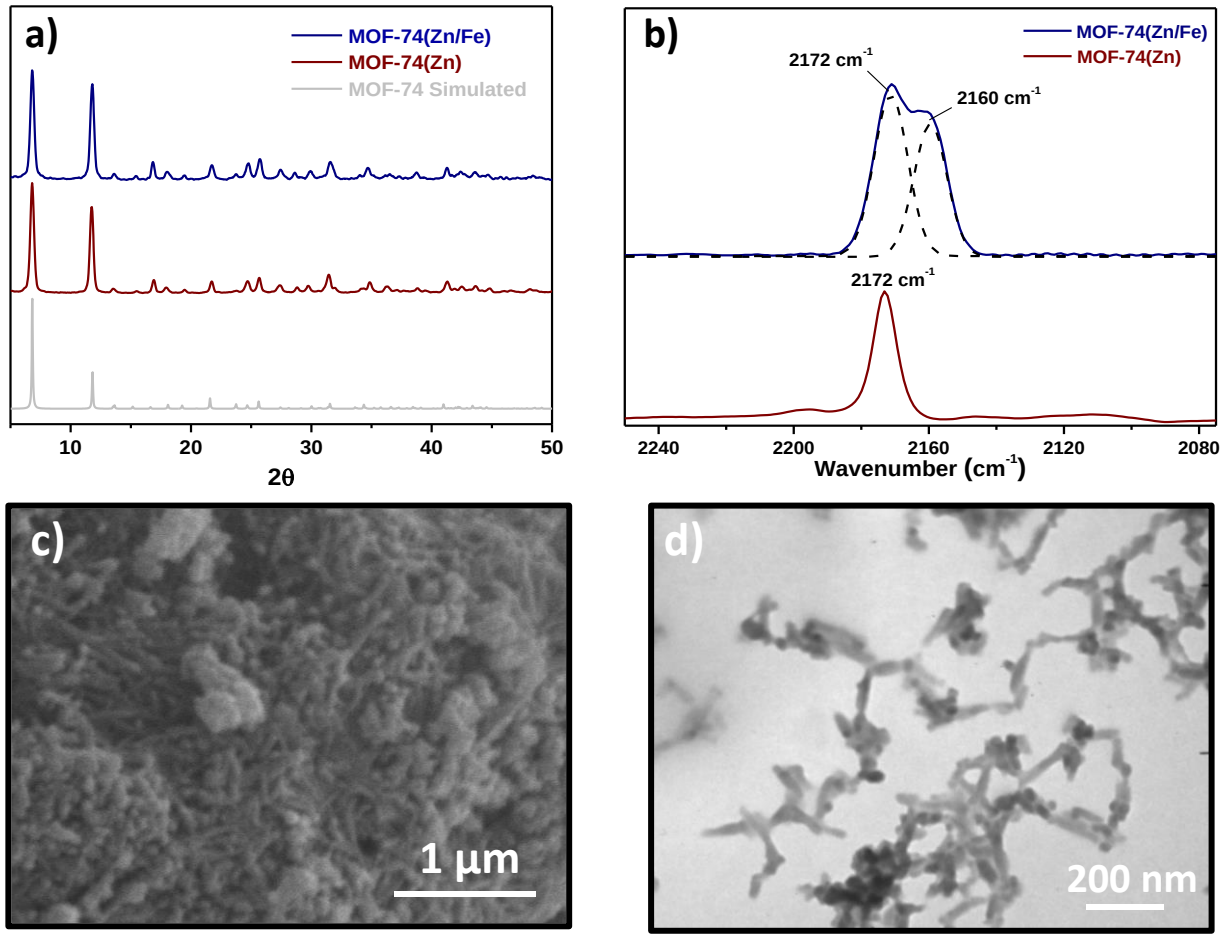

Figure 2. (a) XRD patterns of the MOF-74(Zn/Fe) and MOF-74(Zn) samples. (b) FTIR spectra of CO adsorbed at 100 K on MOF-74(Zn/Fe) and MOF-74(Zn). (c) SEM and (d) TEM images of MOF-74(Zn/Fe).

The composition of the obtained porous carbon materials was analyzed by EDS (Figure S3). The results showed that after the carbonization process, in both cases, homogeneous materials were obtained and no zinc was detected. In the case of C-MOF-74(Zn/Fe) material, the EDS spectra

showed three signals centered at 0.70, 6.40 and 7.0 KeV, which can be assigned to L_{α}, K_{α} and K_{β} peaks of iron, respectively, indicating the presence of iron particles in the C-MOF-74(Zn/Fe) carbon. Thermogravimetric analysis in air at 800 ºC corroborated this result (Figure S4), showing residual weights values of 35 and 0 wt% for C-MOF-74(Zn/Fe) and C-MOF-74(Zn) materials, respectively. The morphology of the obtained carbons was examined by scanning and transmission electron microscopy (Figure 3b-c and Figure S5). As can be seen in the micrographs, both, C-MOF-74(Zn/Fe) and C-MOF-74(Zn), materials retained the nanorod morphology of the precursor MOFs after the carbonization process [50, 59].

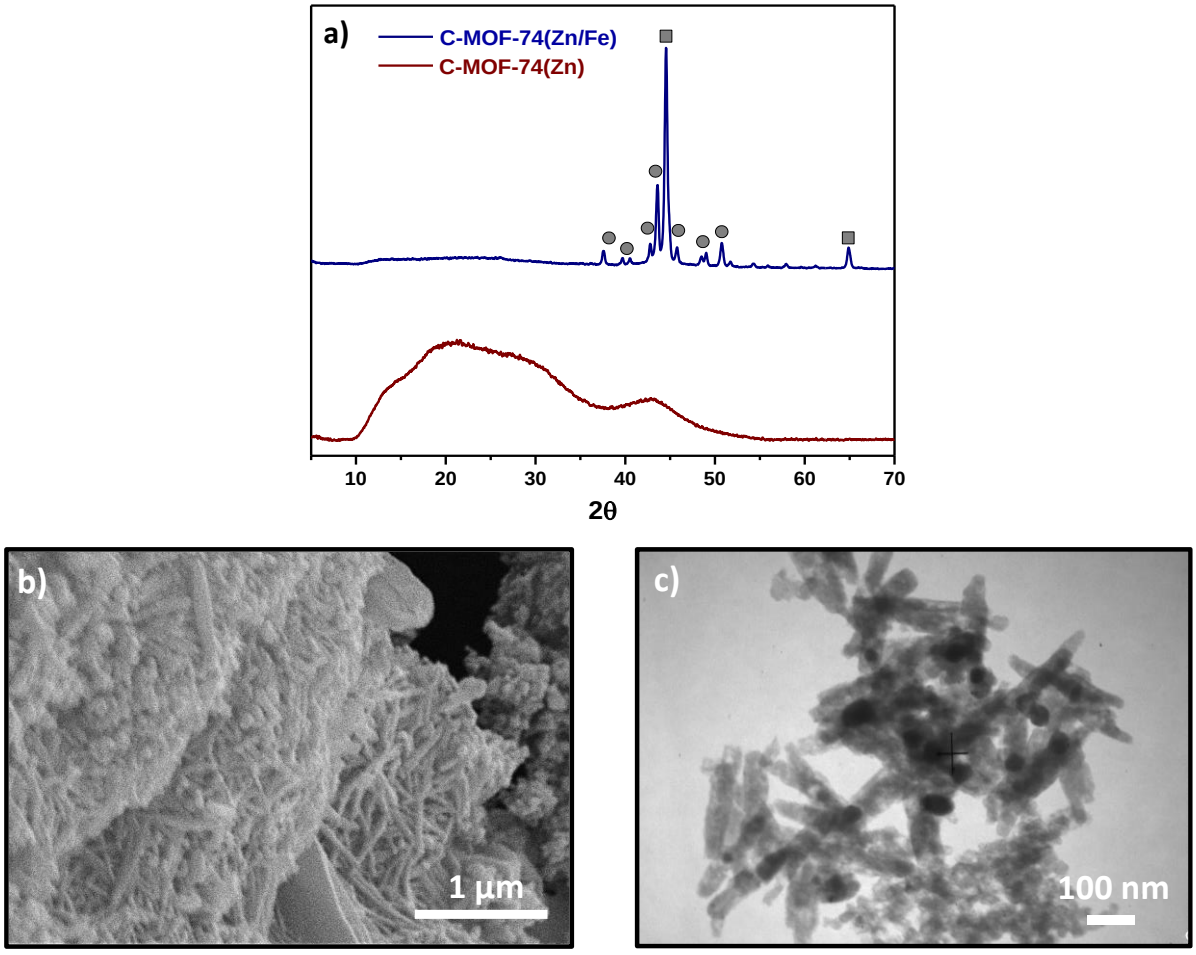

Figure 3. (a) XRD patterns of the C-MOF-74(Zn/Fe) and C-MOF-74(Zn) samples. Peaks: bcc α-Fe (squares), iron carbide (circles). (b) SEM and (c) TEM images of C-MOF-74(Zn/Fe).

Figure 4a shows nitrogen adsorption-desorption isotherms at 77 K of the obtained carbons. Both materials showed a significant N_2 uptake at low relative pressure ($P/P_0 < 0.1$), which is indicative of the presence of micropores. The C-MOF-74(Zn/Fe) and C-MOF-74(Zn) exhibit BET surface area of 860 and 1280 $m^2\ g^{-1}$ and a total pore volume of 1.4 and 1.5 $cm^3\ g^{-1}$, respectively. The lower nitrogen uptake capacity of the C-MOF-74(Zn/Fe) may be attributed to the partial occupation of the pore cavities with the iron particles. Regarding pore size distribution (Figure 4b), both carbon materials show high portion of pores with a diameter centered near 1 nm and also a significant amount of pores in the mesoporous range with a broad size distribution. As previously reported, these mesopores can be the result of the evaporation of metallic zinc and the formation of different gases (such as CO_2, H_2O and CO) during the carbonization process at high temperatures [36, 60, 61].

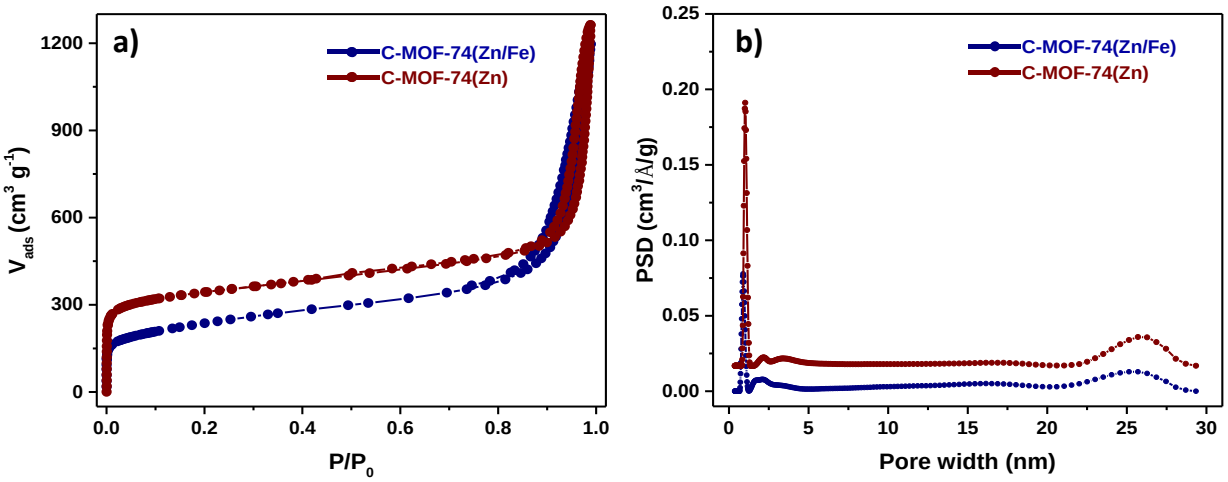

Figure 4. (a) N_2 adsorption-desorption isotherms and (b) pore size distributions of the C-MOF-74(Zn/Fe) and C-MOF-74(Zn) samples.

3.3. Extraction of pollutants from water

To study the potential of the prepared MOF derived carbon nanorods as sorbents of environmental pollutants, methylene blue (MB) and methyl orange (MO), common dye pollutants from the textile and printing industry, were selected as model adsorption analytes. It is worth noting that the obtained C-MOF-74(Zn/Fe), due to the presence of iron particles, shows magnetic properties (Figure S6), which facilitate its retrieval and improves its applicability as sorbent in batch conditions. Figure 5 shows the adsorption isotherms of MB and MO dyes on C-MOF-74(Zn/Fe) and C-MOF-74(Zn) recorded at room temperature after 24 h of adsorption. The adsorption data of MB and MO on C-MOF-74(Zn/Fe) and C-MOF-74(Zn) were fitted by Langmuir model (Figure S7) [51], obtaining high correlation coefficients in all cases (R^2 = 0.999-0.998), which indicates that the Langmuir model was suitable for describing the MB and MO dyes adsorption on both carbon materials. MB and MO have similar dimensions [62], and, given the pore diameters of the obtained carbons, both dyes are able to access the pores of the carbons. However, as can be observed in Figure 5, methylene blue dye was extracted in a higher proportion using both carbon materials. Taking into account the respective cationic and anionic nature of methylene blue and methyl orange [63] and that the isoelectric points were 4.7 for C-MOF-74(Zn/Fe) and 5.2 for C-MOF-74(Zn) (Figure S8), the preferential uptake of MB by both carbon materials can be attributed to the electrostatic attraction between the negatively charged surface of the carbon samples and the positively charged MB at neutral pH. To confirm the important role of the electrostatic interactions in the adsorption of both dyes, the extraction process at different pH values of sample solution was studied (Figure S9). It can be observed that the adsorption of C-MOF-74(Zn/Fe) for MB increased when increasing the pH from 3 to 11, while the MO uptake significantly decreased. In acid conditions, MB and MO are mostly in their neutral form and no electrostatic attraction or repulsion with the positively charged surface of C-MOF-74(Zn/Fe) is expected (Figure S10). In

neutral and basic conditions, dyes are in their ionized form and attractive and repulsive electrostatic interactions can take place between the negatively charged surface of C-MOF-74(Zn/Fe) and the cationic form of MB and anionic form of MO, respectively. The highest MB adsorption and the lowest MO adsorption were obtained at basic pH due to the increment in the negative charge of the carbon surface (Figure S8). However, although the obtained results suggest that electrostatic interactions play a key role in the adsorption of the studied dyes, the high extraction capacity obtained for MO at pH 11 and for MB at pH 3, when electrostatic repulsion and no electrostatic attraction are expected with the carbon materials, respectively, suggest that the adsorption of the dyes by the prepared carbons there must be favored also by other mechanisms, such as π-π interactions (Figure S11). Similar results have been previously reported for this type of carbon materials [47, 64-66].

Comparing the dye extraction performance of both carbon materials, higher dye uptakes were obtained using C-MOF-74(Zn) sample, which could be attributed to its higher surface area. However, after the extraction in dispersive mode, the magnetic properties of C-MOF-74(Zn/Fe) allow the efficient sorbent retrieval from the solution by simply applying an external magnetic field, avoiding tedious filtration and centrifugation procedures. Thus, from the practical application point of view, C-MOF-74(Zn/Fe) material was selected as optimum sorbent for further experiments. It should be noted that the maximum adsorption capacity of methylene blue (370 mg g^{-1}) and methyl orange (239 mg g^{-1}) of the C-MOF-74(Zn/Fe) are comparable or even better than most of the values of adsorption capacity of these dyes reported in the literature using magnetic sorbents, with the additional advantage that they can be obtained from the precursor MOF in a single step (Table S1).

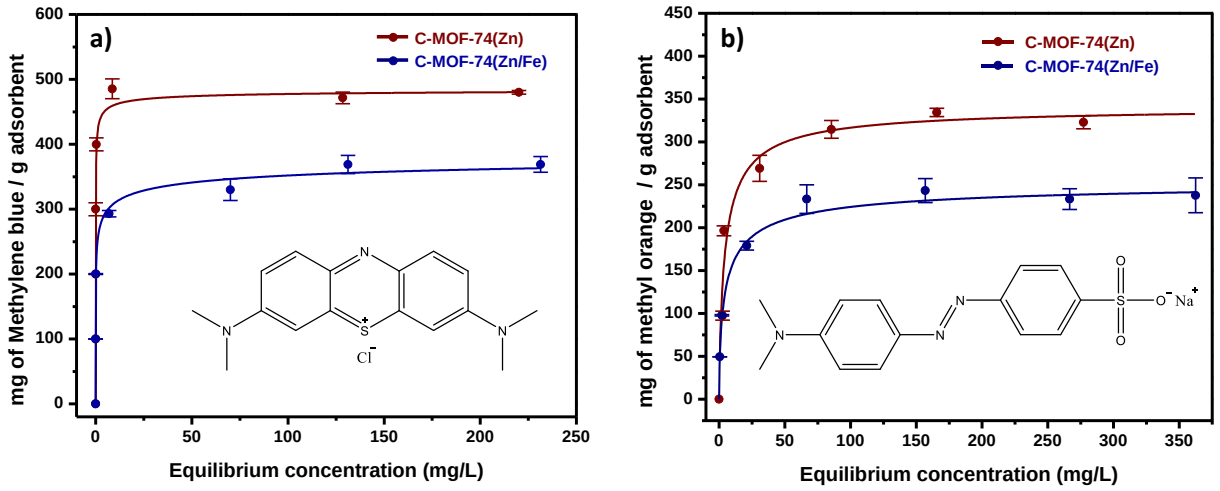

Figure 5. Adsorption isotherms of (a) methylene blue and (b) methyl orange on C-MOF-74(Zn/Fe) and C-MOF-74(Zn). Extraction conditions: 10 mg of carbon; pH 7.0; 10 mL of dye solution; stirring speed of 500 rpm; room temperature; 24 h of extraction time.

The reusability of the sorbent is considered a key factor for application to actual wastewater treatment. Consequently, the reusability of C-MOF-74(Zn/Fe) carbon was evaluated by performing five consecutive extraction cycles of both dye pollutants. After each extraction, the sorbent was washed with 3 x 4 mL of DMF before reuse. As can be seen in Figure 6, C-MOF-74(Zn/Fe) was satisfactorily reused for at least 5 dye adsorption cycles, obtaining variations of just a 0.6 and 1.8 % (expressed as RSD, %) for methylene blue and methyl orange, respectively.

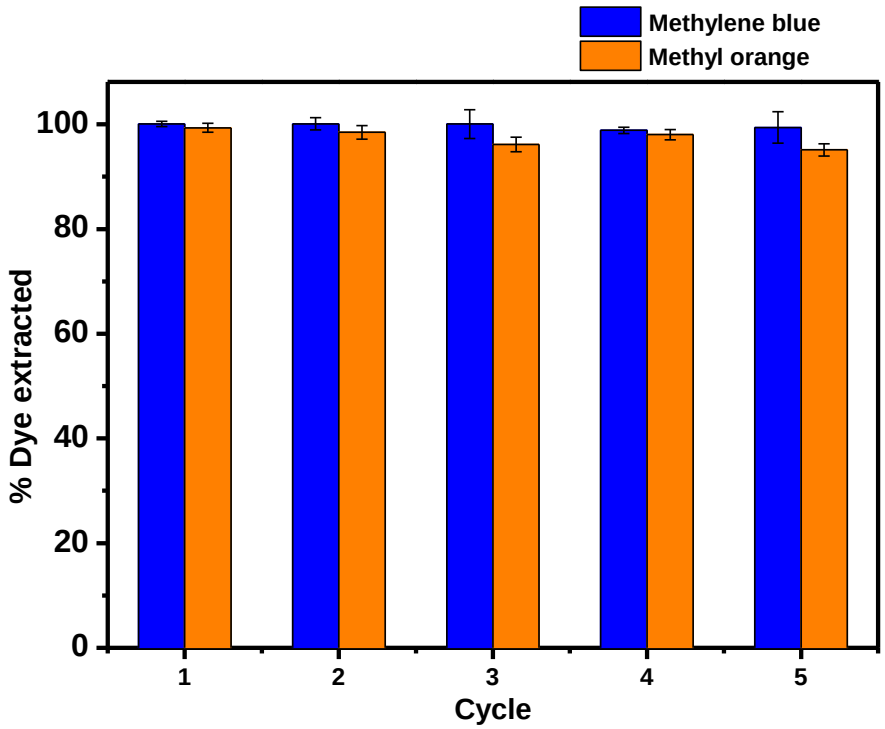

Figure 6. Reusability of C-MOF-74(Zn/Fe) for removal of methylene blue and methyl orange dyes. Extraction conditions: 10 mg of carbon; pH 7.0; 10 mL of dye solution; stirring speed of 500 rpm; room temperature; 24 h of extraction time; C_{dye} = 50 mg L^{-1}.

As an example of practical application, and in order to study the potential matrix effect, the extraction performance of methylene blue was carried using groundwater real samples, which were collected from private wells located in Mallorca Island (Spain). As MB was not detected in the samples, it was spiked. The results are shown in Table 1. As can be observed, the prepared C-MOF-74(Zn/Fe) shows in all cases a high MB extraction capacity (values ranging from 337 to 350 mg g^{-1}) like in distilled water, indicating that there is no significant matrix effect and demonstrating its applicability to treat real samples.

Table 1. Evaluation of the extraction of MB in groundwater samples.

Sample	pH	Conductivity ($\mu S\ cm^{-1}$)	MB added ($mg\ L^{-1}$)	MB measured after removal ($mg\ L^{-1}$)	MB extracted ($mg\ g^{-1}$)
Groundwater 1	7.8	846	400	63.3±6.4	337
Groundwater 2	7.5	1582	400	50.4±13.0	350
Groundwater 3	7.4	1039	400	59.8±4.2	340

Extraction conditions: 10 mg of carbon; 10 mL of dye solution; stirring speed of 500 rpm; room temperature; 24 h of extraction time.

Furthermore, an important feature in the design of adsorbents for environmental pollutant extraction is the ability to treat large volumes of water. This aspect was evaluated carrying out the treatment of 5 L of water polluted with MB (1 ppm) using C-MOF-74(Zn/Fe) material. It was found that the material was able to extract most of the dye (92%) using a very low amount of material (20 mg) (Figure S12).

Considering that multiple pollutants can coexist in real water samples, we also studied the performance of the prepared magnetic porous carbon for the simultaneous extraction of bisphenol A, and two alkylphenols, 4-tert-butylphenol and 4-tert-octylphenol, which have been classified as endocrine disrupting compounds [67, 68]. Figure 7 shows the performance of the C-MOF-74(Zn/Fe) material for the extraction of the selected phenolic pollutants, which were analyzed by HPLC. As can be observed, high extraction percentages (ranging from 95 to 100 %) were obtained for the three studied phenols, which is probably due to the existence of π-π interactions between

the aromatic rings of the phenolic compounds and the C-MOF-74(Zn/Fe) carbon [41, 67]. These results confirmed the potential of the developed C-MOF-74(Zn/Fe) magnetic porous carbon for the removal of environmental pollutants.

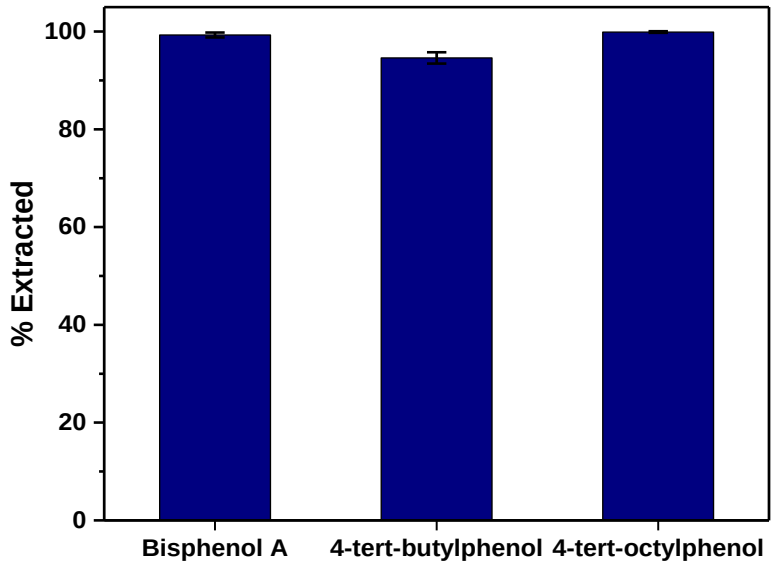

Figure 7. Extraction performance of the C-MOF-74(Zn/Fe) carbon for three phenolic compounds. Extraction conditions: 10 mg of carbon; pH 7.0; 10 mL of phenolic solution; stirring speed of 500 rpm; room temperature; 24 h of extraction time; C_{phenol} = 50 mg L^{-1}, each.

4. CONCLUSIONS

In this work, a highly porous magnetic carbon with nanorod morphology was prepared by a simple calcination of zinc/iron mixed MOF-74. The developed carbon exhibited high surface area (860 $m^2\ g^{-1}$) and pore volume (1.4 $cm^3\ g^{-1}$), with the coexistence of micropores and mesopores. The C-MOF-74(Zn/Fe) was used as an efficient adsorbent for cationic (methylene blue) and anionic (methyl orange) dyes in batch conditions, obtaining maximum adsorption capacities of 370 and 239 mg g^{-1}, respectively, with the advantage of the easy retrieval of the sorbent from water sample by simply applying an external magnetic field. Both electrostatic and π-π interactions played an important role in the dyes removal by C-MOF-74(Zn/Fe). Furthermore, the magnetic carbon could

be reused efficiently over five adsorption cycles and used to treat large volumes of samples. In addition, the obtained material showed good performance for the extraction of MB dye in real water samples and exhibited excellent features to the simultaneous extraction of phenolic compounds, demonstrating that the developed C-MOF-74(Zn/Fe) is a versatile material that can be used as a promising sorbent for the removal of various organic pollutants from water. Finally, it should be noted that the developed approach can be applied using different mixed-metal organic frameworks as precursors for the preparation of other porous carbons with novel structures and properties and great potential in a large number of applications in different fields.

ACKNOWLEDGEMENTS

Spanish Agencia Estatal de Investigación (AEI-Spain) is gratefully acknowledged for financial support through Project PID2019-107604RB-I00/AEI/10.13039/501100011033. M. del Rio acknowledges the support from the Conselleria d'Innovació, Recerca i Turisme (pre-doctoral fellowship). The authors acknowledge F. Hierro Riu for scanning and transmission micrographs.

Declarations of interest: none.

REFERENCES

[1] J. Rivera-Utrilla, M. Sánchez-Polo, M.A. Ferro-García, G. Prados-Joya, R. Ocampo-Pérez, Pharmaceuticals as emerging contaminants and their removal from water. A review, Chemosphere 93 (2013) 1268–1287. https://doi.org/10.1016/j.chemosphere.2013.07.059.

[2] S.D. Richardson, T.A. Ternes, Water analysis: Emerging contaminants and current issues, Anal. Chem. 86 (2014) 2813–2848. https://doi.org/10.1021/acs.analchem.7b04577.

[3] W. Zhang, F. Jiang, Membrane fouling in aerobic granular sludge (AGS)-membrane bioreactor (MBR): Effect of AGS size, Water Res. 157 (2019) 445–453. https://doi.org/10.1016/j.watres.2018.07.069.

[4] W. Chen, J. Mo, X. Du, Z. Zhang, W. Zhang, Biomimetic dynamic membrane for aquatic dye removal, Water Res. 151 (2019) 243–251. https://doi.org/10.1016/j.watres.2018.11.078.

[5] W. Zhang, W. Liang, Z. Zhang, T. Hao, Aerobic granular sludge (AGS) scouring to mitigate membrane fouling: Performance, hydrodynamic mechanism and contribution quantification model, Water. Res. 188 (2021) 116518. https://doi.org/10.1016/j.watres.2020.116518.

[6] M. Al-Harahsheh, M. Aljarrah, M. Alrebaki, M. Mayyas, Nanoionic exchanger with unprecedented loading capacity of uranium, Sep. Purif. Technol. 238 (2020) 116423. https://doi.org/10.1016/j.seppur.2019.116423.

[7] M. Al-Harahsheh, M. Aljarrah, M. Mayyas, M. Alrebaki, High-stability polyamine/amide-functionalized magnetic nanoparticles for enhanced extraction of uranium from aqueous solutions, J. Taiwan Inst. Chem. Eng. 86 (2018) 148–157. https://doi.org/10.1016/j.jtice.2018.03.005.

[8] M.T. Aljarrah, M.S. Al-harahsheh, M.A. Alrebaki, M. Mayyasm, Concentrative isolation of uranium traces in aqueous solutions via resurfaced-magnetic carbon nanotube suspension, J. Environ. Manag. 271 (2020) 110970. https://doi.org/10.1016/j.jenvman.2020.110970.

[9] H. Ren, X. Jin, C. Li, T. Li, Y. Liu, R. Zhou, Rosmarinic acid enhanced Fe(III)-mediated Fenton oxidation removal of organic pollutants at near neutral pH, Sci. Total Environ. 736 (2020) 139528. https://doi.org/10.1016/j.scitotenv.2020.139528.

[10] X. Ren, X. Xu, Y. Xiao, W. Chen, K. Song, Effective removal by coagulation of contaminants in concentrated leachate from municipal solid waste incineration power plants, Sci. Total Environ. 685 (2019) 392–400. https://doi.org/10.1016/j.scitotenv.2019.05.392.

[11] S.Y. Mendiola-Alvarez, J. Araña, J.M.D. Rodríguez, A. Hernández-Ramírez, G.T. Palomino, C.P. Cabello, L. Hinojosa- Reyes, J. Environ. Chem. Eng. 9 (2021) 104828. https://doi.org/10.1016/j.jece.2020.104828.

[12] A. Alsbaiee, B.J. Smith, L. Xiao, Y. Ling, D.E. Helbling, W.R. Dichtel, Rapid removal of organic micropollutants from water by a porous β-cyclodextrin polymer, Nature 529 (2016) 190−194. https://doi.org/10.1038/nature16185.

[13] M. Li, J. Wang, C. Jiao, C. Wang, Q. Wu, Z. Wang, Graphene oxide framework. An adsorbent for solid phase extraction of phenylurea herbicides from water and celery samples, J. Chromatogr. A 1469 (2016) 17−24. https://doi.org/10.1016/j.chroma.2016.09.056.

[14] O.M. Rodriguez-Narvaez, J.M. Peralta-Hernandez, A. Goonetilleke, E.R. Bandala, Treatment technologies for emerging contaminants in water: A review, Chem. Eng. J. 323 (2017) 361−380. https://doi.org/10.1016/j.cej.2017.04.106.

[15] P. Samanta, A.V. Desai, S. Let, S.K. Ghosh, Advanced porous materials for sensing, capture and detoxification of organic pollutants toward water remediation, ACS Sustainable Chem. Eng. 7 (2019) 7456−7478. https://doi.org/10.1021/acssuschemeng.9b00155.

[16] N. Jiang, R. Shang, S.G.J. Heijman, L.C. Rietveld, High-silica zeolites for adsorption of organic micro-pollutants in water treatment: A review, Water Res. 144 (2018) 145−161. https://doi.org/10.1016/j.watres.2018.07.017.

[17] I. Cabrita, B. Ruiz, A.S. Mestre, I.M. Fonseca, A.P. Carvalho, C.O. Ania, Removal of an analgesic using activated carbons prepared from urban and industrial residues, Chem. Eng. J. 163 (2010) 249−255. https://doi.org/10.1016/j.cej.2010.07.058.

[18] J.A.S. Costa, R.A. de Jesus, D.O. Santos, J.F. Mano, L.P.C. Romao, C.M. Paranhos, Recent progresses in the adsorption of organic, inorganic, and gas compounds by MCM-41-based mesoporous materials, Microporous Mesoporous Mater. 291 (2020) 109698. https://doi.org/10.1016/j.micromeso.2019.109698.

[19] N.K. Lazaridis, T.D. Karapantsios, D. Georgantas, Kinetic analysis for the removal of a reactive dye from aqueous solution onto hydrotalcite by adsorption, Water Res. 37 (2003) 3023−3033. https://doi.org/10.1016/S0043-1354(03)00121-0.

[20] Z. Hasan, S.H. Jhung, Removal of hazardous organics from water using metal-organic frameworks (MOFs): Plausible mechanisms for selective adsorptions, J. Hazard. Mater. 283 (2015) 329−339. https://doi.org/10.1016/j.jhazmat.2014.09.046.

[21] Q. Huang, K. Chai, L. Zhou, H. Ji, A phenyl-rich β-cyclodextrin porous crosslinked polymer for efficient removal of aromatic pollutants: Insight into adsorption performace and mechanism, Chem. Eng. J. 387 (2020) 124020. https://doi.org/10.1016/j.cej.2020.124020.

[22] Y. Dai, N. Zhang, C. Xing, Q. Cui, Q. Sun, The adsorption, regeneration and engineering applications of biochar for removal organic pollutants: A review, Chemosphere 223 (2019) 12−27. https://doi.org/10.1016/j.chemosphere.2019.01.161.

[23] J.L.C. Rowsell, O.M. Yaghi, Metal-organic frameworks: a new class of porous materials, Microporous Mesoporous Mater. 73 (2004) 3−14. https://doi.org/10.1016/j.micromeso.2004.03.034.

[24] H. Furukawa, K.E. Cordova, M. O'Keeffe, O.M. Yaghi, The chemistry and applications of metal-organic frameworks, Science, 341 (2013) 1230444. https://doi.org/10.1126/science.1230444.

[25] S.T. Meek, J.A. Greathouse, M.D. Allendorf, Metal-organic frameworks: a rapidly growing class of versatile nanoporous materials, Adv. Mater. 23 (2011) 249−267. https://doi.org/10.1002/adma.201002854.

[26] Y. Cui, B. Li, H. He, W. Zhou, B. Chen, G. Qian, Metal-organic frameworks as platforms for functional materials, Acc. Chem. Res. 49 (2016) 483−493. https://doi.org/10.1021/acs.accounts.5b00530.

[27] S. Abednatanzi, P.G. Derakhshandeh, H. Depauw, F.X. Coudert, H. Vrielinck, P. Van Der Voort, K. Leus, Mixed-metal metal-organic frameworks, Chem. Soc. Rev. 48 (2019) 2535−2565. https://doi.org/10.1039/C8CS00337H.

[28] Y. Pi, X. Li, Q. Xia, J. Wu, Y. Li, J. Xiao, Z. Li, Adsorptive and photocatalytic removal of persistent organic pollutants (POPs) in water by metal-organic frameworks (MOFs), Chem. Eng. J. 337 (2018) 351−371. https://doi.org/10.1016/j.cej.2017.12.092.

[29] Q. Gao, J. Xu, X.H. Bu, Recent advances about metal-organic frameworks in the removal of pollutants from wastewater, Coord. Chem. Rev. 378 (2019) 17−31. https://doi.org/10.1016/j.ccr.2018.03.015.

[30] M.R. Azhar, H.R. Abid, H. Sun, V. Periasamy, M.O. Tadé, S. Wang, One-pot synthesis of binary metal organic frameworks (HKUST-1 and UiO-66) for enhanced adsorptive

removal of water contaminants, J. Colloid Interface Sci. 490 (2017) 685–694. https://doi.org/10.1016/j.jcis.2016.11.100.

[31] S. Zhong, C. Zhan, D. Cao, Zeolitic imidazolate framework-derived nitrogen-doped porous carbons as high performance supercapacitor electrode materials, Carbon, 85 (2015) 51–59. https://doi.org/10.1016/j.carbon.2014.12.064.

[32] W. Yang, X. Li, Y. Li, R. Zhu, H. Pang, Applications of metal-organic framework-derived carbon materials, Adv. Mater. 31 (2019) 1804740. https://doi.org/10.1002/adma.201804740.

[33] C. Wang, J. Kim, J. Tang, M. Kim, H. Lim, V. Malgras, J. You, Q. Xu, J. Li, Y. Yamauchi, New strategies for novel MOF-derived carbon materials based on nanoarchitectures, Chem 6 (2020) 19–40. https://doi.org/10.1016/j.chempr.2019.09.005.

[34] M. Hu, J. Reboul, S. Furukawa, N.L. Torad, Q. Ji, P. Srinivasu, K. Ariga, S. Kitagawa, Y. Yamauchi, Direct carbonization of Al-based porous coordination polymer for synthesis of nanoporous carbon, J. Am. Chem. Soc. 134 (2012) 2864–2867. https://doi.org/10.1021/ja208940u.

[35] X. Yan, X. Li, Z. Yan, S. Komarneni, Porous carbons prepared by direct carbonization of MOFs for supercapacitors, Appl. Surf. Sci. 308 (2014) 306–310. https://doi.org/10.1016/j.apsusc.2014.04.160.

[36] Z. Abbasi, E. Shamsaei, S.K. Leong, B. Ladewig, X. Zhang, H. Wang, Effect of carbonization temperature on adsorption property of ZIF-8 derived nanoporous carbon for water treatment, Microporous Mesoporous Mater. 236 (2016) 28–37. https://doi.org/10.1016/j.micromeso.2016.08.022.

[37] S. Xu, Y. Lv, X. Zeng, D. Cao, ZIF-derived nitrogen-doped porous carbons as highly efficient adsorbents for removal of organic compounds from wastewater, Chem. Eng. J. 323 (2017) 502–511. https://doi.org/10.1016/j.cej.2017.04.093.

[38] M. Sarker, I. Ahmed, S.H. Jhung, Adsorptive removal of herbicides from water over nitrogen-doped carbon obtained from ionic liquid@ZIF-8, Chem. Eng. J. 323 (2017) 203–211. https://doi.org/10.1016/j.cej.2017.04.103.

[39] I. Ahmed, B.N. Bhadra, H.J. Lee, S.H. Jhung, Metal-organic framework-derived carbons: Preparation from ZIF-8 and applicaction in the adsorptive removal of sulfamethoxazole from water, Catal. Today 301 (2018) 90–97. https://doi.org/10.1016/j.cattod.2017.02.011.

[40] S. Li, X. Zhang, Y. Huang, Zeolitic imidazolate framework-8 derived nanoporous carbon as an effective and recyclable adsorbent for removal of ciprofloxacin antibiotics from water, J. Hazard. Mater. 321 (2017) 711–719. https://doi.org/10.1016/j.jhazmat.2016.09.065.

[41] B.N. Bhadra, S.H. Jhung, A remarkable adsorbent for removal of contaminants of emerging concern from water: Porous carbon derived from metal azolate framework-6, J. Hazard. Mater. 340 (2017) 179–188. https://doi.org/10.1016/j.jhazmat.2017.07.011.

[42] B.N. Bhadra, J.K. Lee, C.W. Cho, S.H. Jhung, Remarkably efficient adsorbent for the removal of bisphenol A from water: Bio-MOF-1-derived porous carbon, Chem. Eng. J. 343 (2018) 225–234. https://doi.org/10.1016/j.cej.2018.03.004.

[43] D. Chen, H. Sun, Y. Wang, H. Quan, Z. Ruan, Z. Ren, X. Luo, UiO-66 derived zirconia/porous carbon nanocomposites for efficient removal of carbamazepine and adsorption mechanism, Appl. Surf. Sci. 507 (2020) 145054. https://doi.org/10.1016/j.apsusc.2019.145054.

[44] C.P. Cabello, M.F.F. Picó, F. Maya, M. del Rio, G.T. Palomino, UiO-66 derived etched carbon/polymer membranes: High-performance supports for the extraction of organic pollutants from water, Chem. Eng. J. 346 (2018) 85–93. https://doi.org/10.1016/j.cej.2018.04.019.

[45] N.C. Sánchez, J.L. Guzmán-Mar, L. Hinojosa-Reyes, G.T. Palomino, C.P. Cabello, Carbon composite membrane derived from MIL-125-NH_2 MOF for the enhanced extraction of emerging pollutants, Chemosphere 231 (2019) 510–517. https://doi.org/10.1016/j.chemosphere.2019.05.173.

[46] N.L. Torad, M. Hu, S. Ishihara, H. Sukegawa, A.A. Belik, M. Imura, K. Ariga, Y. Sakka, Y. Yamauchi, Direct synthesis of MOF-derived nanoporous carbon with magnetic Co nanoparticles toward efficient water treatment, Small 10 (2014) 2096–2107. https://doi.org/10.1002/smll.201302910.

[47] A. Banerjee, R. Gokhale, S. Bhatnagar, J. Jog, M. Bhardwaj, B. Lefez, B. Hannoyer, S. Ogale, MOF derived porous carbon-Fe_3O_4 nanocomposite as a high performance recyclable environmental superadsorbent, J. Mater. Chem. 22 (2012) 19694–19699. https://doi.org/10.1039/C2JM33798C.

[48] D. Chen, C. Chen, W. Shen, H. Quan, S. Chen, S. Xie, X. Luo, L. Guo, MOF-derived magnetic porous carbon-based sorbent: Synthesis, characterization, and adsorption behaviour of organic micropollutants, Adv. Powder Technol. 28 (2017) 1769–1779. https://doi.org/10.1016/j.apt.2017.04.018.

[49] F. Yu, H. Zhou, Q. Shen, Modification of cobalt-containing MOF-derived mesoporous carbon as an effective sulfur-loading host for rechargeable lithium-sulfur batteries, J. Alloys Compd. 772 (2019) 843–851. https://doi.org/10.1016/j.jallcom.2018.09.103.

[50] P. Pachfule, D. Shinde, M. Majumder, Q. Xu, Fabrication of carbon nanorods and graphene nanoribbons from a metal-organic framework, Nat. Chem. 8 (2016) 718–724. https://doi.org/10.1038/nchem.2515.

[51] K.Y. Foo, B.H. Hameed, Insights into the modeling of adsorption isotherm systems, Chem. Eng. J. 156 (2010) 2–10. https://doi.org/10.1016/j.cej.2009.09.013.

[52] N.L. Rosi, J. Kim, M. Eddaoudi, B. Chen, M. O'Keeffe, O.M. Yaghi, Rod packing and metal-organic frameworks constructed from rod-shaped secondary building units, J. Am. Chem. Soc. 127 (2005) 1504–1518. https://doi.org/10.1021/ja045123o.

[53] E.D. Bloch, M.R. Hudson, J.A. Mason, S. Chavan, V. Crocellà, J.D. Howe, K. Lee, A.L. Dzubak, W.L. Queen, J.M. Zadrozny, S.J. Geier, L.C. Lin, L. Gagliardi, B. Smit, J.B. Neaton, S. Bordiga, C.M. Brown, J.R. Long, Reversible CO binding enables tunable CO/H_2 and CO/N_2 separations in metal-organic frameworks with exposed divalent metal cations, J. Am. Chem. Soc. 136 (2014) 10752–10761. https://doi.org/10.1021/ja505318p.

[54] Y. Hou, T. Huang, Z. Wen, S. Mao, S. Cui, J. Chen, Metal-organic framework-derived nitrogen-doped core-shell-structured porous Fe/Fe_3C@C nanoboxes supported on graphene sheets for efficient oxygen reduction reactions, Adv. Energy Mater. 4 (2014) 1400337. https://doi.org/10.1002/aenm.201400337.

[55] R. Qiang, Y. Du, H. Zhao, Y. Wang, C. Tian, Z. Li, X. Han, P. Xu, Metal organic framework-derived Fe/C nanocubes toward efficient microwave absorption, J. Mater. Chem. A 3 (2015) 13426−13434. https://doi.org/10.1039/C5TA01457C.

[56] M. Al-Harahsheh, Thermodynamic analysis on the thermal treatment of electric arc furnace dust-PVC blends, Arab. J. Sci. Eng. 43 (2018) 5757−5769. https://doi.org/10.1007/s13369-017-2994-0.

[57] M. Al-Harahsheh, A. Al-Otoom, M. Al-Jarrah, M. Altarawneh, S. Kingman, Thermal análisis on the pyrolysis of tetrabromobisphenol A and electric arc furnace dust mixtures, Metall. Mater. Trans. B 49 (2018) 45−60. https://doi.org/10.1007/s11663-017-1121-7.

[58] S. Mukherjee, D.A. Cullen, S. Karakalos, K. Liu, H. Zhang, S. Zhao, H. Xu, K.L. More, G. Wang, G. Wu, Metal-organic framework-derived nitrogen-doped highly disordered carbon for electrochemical ammonia synthesis using N_2 and H_2O in alkaline electrolytes, Nano Energy 48 (2018) 217−226. https://doi.org/10.1016/j.nanoen.2018.03.059.

[59] S. Dang, Q.L. Zhu, Q. Xu, Nanomaterials derived from metal-organic frameworks, Nat. Rev. Mater. 3 (2018) 17075. https://doi.org/10.1038/natrevmats.2017.75.

[60] L. Ye, G. Chai, Z. Wen, Zn-MOF-74 derived N-doped mesoporous carbon as pH-universal electrocatalyst for oxygen reduction reaction, Adv. Funct. Mater. 27 (2017) 1606190. https://doi.org/10.1002/adfm.201606190.

[61] A.D. Tan, K. Wan, Y.F. Wang, Z.Y. Fu, Z.X. Liang, N,S-containing MOF-derived dual-doped mesoporous carbon as a highly effective oxygen reduction reaction electrocatalyst, Catal. Sci. Technol. 8 (2018) 335−343. https://doi.org/10.1039/C7CY02265D.

[62] Q. Yang, S. Ren, Q. Zhao, R. Lu, C. Hang, Z. Chen, H. Zheng, Selective separation of methyl orange from water using magnetic ZIF-67 composites, Chem. Eng. J. 333 (2018) 49−57. https://doi.org/10.1016/j.cej.2017.09.099.

[63] Y.Y. Lau, Y.S. Wong, T.T. Teng, N. Morad, M. Rafatullah, S.A. Ong, Degradation of cationic and anionic dyes in coagulation-flocculation process using bi-functionalized silica hybrid with aluminum-ferric as auxiliary agent, RSC Adv. 5 (2015) 34206−34215. https://doi.org/10.1039/C5RA01346A.

[64] F. Yu, X. Bai, M. Liang, J. Ma, Recent progess on metal-organic framework-derived porous carbon and its composite for pollutant adsorption from liquid phase, Chem. Eng. J. 405 (2021) 126960. https://doi.org/10.1016/j.cej.2020.126960.

[65] K.C. Bedin, A.C. Martins, A.L. Cazetta, O. Pezoti, V.C. Almeida, KOH-activated carbon prepared from sucrose spherical carbon: Adsorption equilibrium, kinetic and thermodynamic studies for Methylene Blue removal, Chem. Eng. J. 286 (2016) 476–484. https://doi.org/10.1016/j.cej.2015.10.099.

[66] J. Ye, L. Jin, X. Zhao, X. Qian, M. Dong, Superior adsorption performance of metal-organic-frameworks derived magnetic cobalt-embedded carbon microrods for triphenylmethane dyes, J. Colloid Interface Sci. 536 (2019) 483–492. https://doi.org/10.1016/j.jcis.2018.10.073.

[67] M.B. Ahmed, J.L. Zhou, H.H. Ngo, M.A.H. Johir, K. Sornalingam, Sorptive removal of phenolic endocrine disruptors by functionalized biochar: Competitive interaction mechanism, removal efficacy and application in wastewater, Chem. Eng. J. 335 (2018) 801–811. https://doi.org/10.1016/j.cej.2017.11.041.

[68] S. Dhaka, R. Kumar, A. Deep, M.B. Kurade, S.W. Ji, B.H. Jeon, Metal-organic frameworks (MOFs) for the removal of emerging contaminants from aquatic environments, Coord. Chem. Rev. 380 (2019) 330–352. https://doi.org/10.1016/j.ccr.2018.10.003.